Estimating habitat volume of living resources using three-dimensional circulation and biogeochemical models

Katharine A. Smith[a,1,*], Zachary Schlag[b], and Elizabeth W. North[c]

[a] University of Maryland Center for Environmental Science Horn Point Laboratory, P.O. Box 775, Cambridge, MD 21613, USA [email: kasmith6@hawaii.edu].

[b] University of Maryland Center for Environmental Science Horn Point Laboratory, P.O. Box 775, Cambridge, MD 21613, USA [email: zachary.schlag@gmail.com].

[c] University of Maryland Center for Environmental Science Horn Point Laboratory, P.O. Box 775, Cambridge, MD 21613, USA [email: enorth@umces.edu].

[1] Current address: University of Hawaiʻi at Mānoa, 1000 Pope Rd., Honolulu, HI 96822, USA

* Corresponding author: Katharine A. Smith, kasmith6@hawaii.edu

Authorship statements:

K. Smith developed and tested the three different methods for calculating a grid cell volume, helped plan the implementation of the chosen method for estimating habitat volumes, and wrote the bulk of the manuscript.

Z. Schlag implemented the volume algorithm to create a model that evaluates the full habitat volume in a hydrodynamic model and added details to the manuscript.

E. North was a co-PI on the grant that supported this research, and proposed and conceptualized the idea for a model calculating habitat volumes in biogeochemical hydrodynamic models, aided in the planning and testing of this model, and contributed considerably to the manuscript writing.

Abstract

Coupled three-dimensional circulation and biogeochemical models predict changes in water properties that can be used to define fish habitat, including physiologically important parameters such as temperature, salinity, and dissolved oxygen. Yet methods for calculating the volume of habitat defined by the intersection of multiple water properties are not well established for coupled three-dimensional models. The objectives of this research were to examine multiple methods for calculating habitat volume from three-dimensional model predictions, select the most robust approach, and provide an example application of the technique. Three methods were assessed: the “Step,” “Ruled Surface”, and “Pentahedron” methods, the latter of which was developed as part of this research. Results indicate that the analytical Pentahedron method is exact, computationally efficient, and preserves continuity in water properties between adjacent grid cells. As an example application, the Pentahedron method was implemented within the Habitat Volume Model (HabVol) using output from a circulation model with an Arakawa C-grid and physiological tolerances of juvenile striped bass (*Morone saxatilis*). This application demonstrates that the analytical Pentahedron method can be successfully applied to calculate habitat volume using output from coupled three-dimensional circulation and biogeochemical models, and it indicates that the Pentahedron method has wide application to aquatic and marine systems for which these models exist and physiological tolerances of organisms are known.

Keywords

Circulation model; hydrodynamic model; Habitat model; Habitat volume; Physiological tolerances; Biological-physical interactions; Coupled three-dimensional circulation and biogeochemical models

1. Introduction

Numerical circulation models have become important tools in understanding the physical dynamics of oceanic and coastal systems (e.g., Allen et al., 1995; Ezer and Mellor, 1994; Holloway and Merrifield, 1999; Li et al., 2005), and numerical biogeochemical models have played a central role in understanding water quality responses to nutrient loading (e.g., Cerco, 1995; Kremer and Nixon, 1978; Li et al. 2016; Peeters et al., 1995). These models provide greater understanding of the interactions between physical and biological processes and the characteristics of a system, and they can be used to understand past events as well as make future projections, such as the effects of climate change (e.g., Caldeira and Wickett, 2003; Harley et al., 2006; IPCC, 2007; Scavia et al., 2002). In marine ecosystems, physical conditions can have profound effects on the species living there (Mann and Lazier, 2006). In addition, in coastal systems, eutrophication is a widespread problem that is altering estuarine ecosystems and the habitat and nursery areas of many commercially and recreationally important fish species (Caddy, 1993; Karlson et al., 2002; Kemp et al., 2005; Nixon, 1995). Thus, understanding changing physical and biogeochemical conditions can help us predict how each species will be affected by changes in the environment. The goal of this research was to develop and describe a numerical tool that integrates the predictions of three-dimensional numerical circulation and biogeochemical models with organisms' physiological tolerances to quantify how changes in environmental conditions influence the habitat of living marine resources.

Temperature, salinity, and dissolved oxygen (DO) are important factors which influence habitat suitability for fish and invertebrate species (e.g., Hanks and Secor, 2011; McLeese, 1956; Wuenschel et al., 2004). Physiological tolerances to these factors can differ markedly between species that inhabit the same system (e.g., Brandt, 1993; Breitburg, 1994; Diaz and Rosenberg, 1995; Funderburk et al., 1991; Miller et al., 2002; Secor and Gunderson, 1998). Although there are numerous examples of the use of different physiological requirements and numerical models to calculate suitable habitat in two dimensions (e.g., Barnes et al. 2007; Bidegain et al. 2013; Kimmerer et al., 2009; MacWilliams et al., 2016; Yi et al. 2010), fewer efforts have quantified the three-dimensional volume of suitable habitat (but see Cline et al. 2013; Kimmerer et al., 2009; Kimmerer et al. 2013; Mouton et al. 2007; Schlenger et al. 2013b). Because coupled three-dimensional circulation and biogeochemical models can predict changes in various water properties, including temperature, salinity, and DO, in three dimensions over time, the predictions of these models could be used to estimate changes in the volumetric extent of suitable habitat for a given species, with application for understanding how habitat changes from year to year, how eutrophication and climate change could affect habitat, and which species may be most sensitive to these stressors.

The objectives of this study were to examine multiple approaches for calculating habitat volume from three-dimensional model predictions, select the most robust approach, and provide an example application of the technique. Although the algorithms developed herein could be used with numerical model grids based on either quadrilaterals (e.g., curvilinear models) or triangles (e.g., finite element models), the development of methods for calculating habitat volume focused on an Arakawa C-grid, which is the grid structure of the Regional Ocean Modeling System (ROMS) (Song and Haidvogel, 1994) and the Princeton Ocean Model (POM) (Blumberg and Mellor, 1987). Three different techniques to calculate the volume of suitable habitat were tested and compared. The most suitable method was used within the Habitat Volume Model (HabVol) to provide an example of how the algorithm could be implemented and applied to evaluate the habitat of juvenile striped bass (*Morone saxatilis*) in Chesapeake Bay.

2. Methods and Results

2.1. Algorithm development and testing

Three methods for calculating the volume of a grid cell defined by rho nodes of an Arakawa C-grid were investigated: the "Step," "Pentahedron," and "Ruled Surface" methods. In this section, we describe each of the three methods for calculating volume, and then compare them for efficiency and precision. All three methods used a grid structure that placed the rho nodes, where depth and hydrographic parameters including temperature, salinity, and dissolved oxygen were defined, at the vertices of the grid cells used for calculating habitat volume (Fig. 1). Note that in an Arakawa C-grid, rho nodes are located at the center of the grid cells, are distributed non-linearly over the *x*- and *y*-directions, and can occur at multiple varying depths (at s- or sigma-levels). In addition, the vertices of the rho grid cells often are not part of standard model output. The rho nodes were chosen to be the vertices of the grid for volume calculations so that rho-node coordinates would be the only coordinates required for calculations. The calculation of the volume of the resulting grid cells was non-trivial because 1) the curvilinear grid cells do not necessarily contain parallel lines, and 2) the top and bottom faces of the grid cells are not necessarily planar because adjacent rho nodes may be located at different depths (i.e., they are skew quadrilaterals; Fig. 2).

In the Step method, grid cells were interpreted as having flat, horizontal top and bottom faces by averaging the z-coordinates (z) of the top four vertices [(x_1, y_1, z_{t1}), (x_2, y_2, z_{t2}), (x_3, y_3, z_{t3}), (x_4, y_4, z_{t4})] and the bottom four vertices [(x_1, y_1, z_{b1}), (x_2, y_2, z_{b2}), (x_3, y_3, z_{b3}), (x_4, y_4, z_{b4})], respectively (Fig. 3a). The volume was then simply the average height of the cell multiplied by the horizontal cross-sectional area of the cell (A):

$$V = A \times \left[\frac{1}{4}\left(z_{t1} + z_{t2} + z_{t3} + z_{t4}\right) - \frac{1}{4}\left(z_{b1} + z_{b2} + z_{b3} + z_{b4}\right) \right], \qquad (1a)$$

where

$$A = \frac{1}{2}\left|(x_1 y_2 - x_2 y_1) + (x_2 y_3 - x_3 y_2) + (x_3 y_4 - x_4 y_3) + (x_4 y_1 - x_1 y_4)\right|. \qquad (1b)$$

Although this technique was conceptually and computationally simple, it did not allow calculation of continuous surfaces of suitable habitat, because the surfaces of adjacent grid cells were not continuous across multiple grid cells (see Fig. 3a).

The Pentahedron (Fig. 3b) and Ruled Surface (Fig. 3c) methods both allowed for continuity in the physical and chemical characteristics of the water across multiple grid cells. In the Pentahedron method, the top and bottom faces were each divided into four triangles; the vertices of each of these triangles included two adjacent rho nodes at the edges of the face as well as the center point of the face. The grid cell was then divided into four triangular pentahedrons formed by connecting the triangles of the top and bottom faces (Fig. 3b). The total volume (V) of the grid cell was calculated as the sum of the volume of each pentahedron (v_i):

$$V = \sum_{i=1}^{4} v_i. \qquad (2a)$$

The volume of each pentahedron was calculated using the coordinates of the three points at the top [(x_1, y_1, z_{t1}), (x_2, y_2, z_{t2}), (x_3, y_3, z_{t3})] and bottom [(x_1, y_1, z_{b1}), (x_2, y_2, z_{b2}), (x_3, y_3, z_{b3})] of each pentahedron:

$$v_i = \frac{A'}{3}\left[\left(z_{t1} + z_{t2} + z_{t3}\right) - \left(z_{b1} + z_{b2} + z_{b3}\right)\right], \qquad (2b)$$

where A' is the cross sectional area of the pentahedron:

$$A' = \frac{1}{2}\left|x_1\left(y_2 - y_3\right) + x_2\left(y_3 - y_1\right) + x_3\left(y_1 - y_2\right)\right|. \qquad (2c)$$

Hence the "Pentahedron method," which interprets the grid cell as being composed of four pentahedrons, is an exact method based on the geometric solution for the volume of a pentahedron. When applied to a numerical model, the Pentrahedron method is an exact solution for habitat volume in each vertical grid cell as long as the habitat variable varies linearly along the edges of the cell, which is a valid assumption because numerical models cannot predict nonlinear behavior, like temperature inversions, within one vertical grid cell (i.e., between two grid points in the vertical).

In the Ruled Surface method, the top and bottom faces of the grid cell were assumed to be the hyperbolic paraboloids defined by the skew quadrilaterals connecting the rho node vertices of each face. These were doubly ruled surfaces (i.e., through each point on the surface there are two straight lines that lie on the surface) that were formed through bilinear interpolation, presenting one of the smoothest possible interpretations of the grid cell faces. The ruled surface was constructed by drawing lines connecting midpoints of opposite sides of the skew quadrilateral, then connecting matching quarter points, and so forth (Fig. 3c) (Farin, 1996; Wells, 2012). Thus, the z coordinate of the ruled surface of the top face at a horizontal position (x, y) was defined as

$$z_t = \frac{\left[(z_{t4} - z_{t1})(1-s) + (z_{t3} - z_{t2})s\right] \times \left[y - y_1(1-s) - y_2 s\right]}{(y_4 - y_1)(1-s) + (y_3 - y_2)s + z_{t1}(1-s) + z_{t2}s}, \qquad (3a)$$

where s is the fraction of the distance from the side joining (x_1, y_1, z_{t1}) with (x_4, y_4, z_{t4}) to the side joining (x_2, y_2, z_{t2}) with (x_3, y_3, z_{t3}) at which (x, y) is located; that is,

$$s = \frac{-b - \sqrt{b^2 - 4ac}}{2a}, \qquad (3b)$$

where

$$
\begin{aligned}
a &= (y_4 - y_3)(x_1 - x_2) + (x_4 - x_3)(y_2 - y_1) \\
b &= (y_1 - y_4)(x_1 - x_2) + (x_1 - x_4)(y_2 - y_1) + (x - x_1)(y_4 + y_2 - y_1 - y_3) \\
&\quad + (y_1 - y)(x_4 + x_2 - x_1 - x_3) \\
c &= (y_1 - y_4)(x - x_1) + (x_1 - x_4)(y_1 - y)
\end{aligned}
\tag{3c}
$$

The corresponding z coordinate for the bottom face was found with the same equations, replacing the subscript "t" with "b". The volume defined by this method was computed numerically using the statistical programming language R (R Development Core Team, 2005) and excluded rare cases when grid coordinates could lead to zero in the denominator. First, a box defined by the x, y, and z extremes of the grid cell was drawn around the grid cell (outer box in Fig. 4). Then, evenly spaced points in x-y space in the box were sampled to find the grid cell heights at each location (h_i) (dashed lines in Fig. 4), which were calculated as the difference between the z coordinates in the top and bottom faces. An x-y point in the box that was out of the bounds of the grid cell was considered to have a height of zero. The volume (V) of the grid cell was then calculated as

$$
V = \frac{A'}{n} \sum_{i=1}^{n} h_i \tag{4}
$$

where A'' is the horizontal cross-sectional area of the box (Fig. 4) and n is the total number of x-y points sampled. The accuracy of the numerical solution for the volume can be improved by sampling the heights in the grid cell at more closely spaced x-y points. Although this numerical technique was hypothesized to be more precise than the other methods because of increased smoothness of the grid cell top and bottom faces, the iterative numerical nature of the solution was clearly more computationally intensive than the analytical methods.

To determine how the numerical Ruled Surface method compared with the analytical Pentahedron and Step methods, multiple tests of the Ruled Surface method were conducted on a model grid cell using increasing resolution. The goal was to determine the resolution (i.e., the number of *x*-*y* points) needed for the Ruled Surface model to converge on a stable volume and then to compare this volume to the solutions derived from the other two methods. Results of this test indicate that as the resolution was increased, the volume from the Ruled Surface method converged with the volume calculated using the analytical Pentahedron method (Fig. 5). For the test grid cell, the volume calculated with the Step method was slightly larger than that calculated by the other methods.

On a single processor, the mean time (± std, n = 10) to calculate the volume of the grid cell in Fig. 5 was 0.032 ± 0.006, 0.033 ± 0.007, and 3.636 ± 0.044 s for the Step, Pentahedron, and Ruled Surface methods, respectively, with Ruled Surface sampling resolution = 200. The Step method did not offer a significant difference in time efficiency compared to the Pentahedron method, while the time-consuming Ruled Surface method did not offer increased precision compared to the Pentahedron method. Based on these results, the Pentahedron method was selected as the optimal method because it was exact, computationally efficient, and preserved the continuity of surfaces across multiple grid cells.

2.2. Implementation and application

After identifying the Pentahedron method as the most appropriate method for calculating the volume of a grid cell, the next step was to implement the method to calculate the volume of suitable habitat for a marine organism across an entire circulation model domain. First, a method for defining suitable habitat volume within a grid cell based on a species' physiological tolerances was developed. In each grid cell in the model, linear interpolation in the vertical direction was used to find what depths, if any, corresponded to the limits of a species' tolerance to a physical water property (Fig. 6a). These interpolated locations were used in combination with the grid cell nodes where suitable habitat existed to define the border vertices of the region of suitable habitat within the grid cell (Fig. 6b). In the case of multiple constraints (e.g., temperature and salinity), the most limiting vertices defined the borders of the habitat region (Fig. 6a). The Pentahedron method was then used to calculate the volume of the region defined by the border vertices (Fig. 6c). Finally, summing all such volumes from every model grid cell gave the full habitat volume within the model domain (Fig. 6d).

The Pentahedron habitat volume method was incorporated into a stand-alone open source Fortran program that can be applied to calculate habitat volume for species in multiple estuarine and coastal systems. This Habitat Volume Model (HabVol) runs with output from the curvilinear Regional Ocean Modeling System (ROMS) (Schlenger et al. 2013a) and uses the rho nodes of the ROMS model to define the grid vertices of the HabVol model (e.g., Fig. 1). HabVol implements the Pentahedron method to calculate the system-wide suitable habitat for the variables specified by the user, as well as for the intersection of the variables if more than one is specified (e.g., Fig. 6). In implementing this habitat volume method, special treatment was required for horizontal grid locations where no suitable habitat existed (e.g., land, or nodes where no water properties were within the range of a species' physiological tolerances). In these cases, the horizontal grid cells were sectioned as depicted in Fig. 7, using the midpoints between habitat and non-habitat nodes as volume-defining vertices. Equations 2b,c were applied to the pentahedrons defined by the numbered faces in each case shown in Fig. 7, and their volumes were summed.

In addition to calculating habitat volume based on fixed physiological tolerances (e.g., intersections of salinity, temperature, and/or dissolved oxygen), HabVol also can be used to calculate volumes based on bioenergetics (e.g., where potential growth is positive) (Schlenger et al., 2013b). The user can specify a subset of the ROMS model domain in which to calculate habitat volume (e.g., one river system) and can limit the volume calculations to a specified distance from bottom (e.g., the volume of water within 2 m of bottom which meets specified physiological constraints).

As an example of HabVol application, the salinity and temperature ranges that were optimal for growth of juvenile striped bass (*Morone saxatilis*) (Schlenger, 2012) were used to find the optimal habitat based on salinity and temperature separately as well as their intersection using ROMS model predictions for Chesapeake Bay on August 15, 1996. Habitat volumes based individually on optimal salinity range (1–15) and optimal temperature range (24–27 °C) were calculated to be 69.8 km^3 and 103.2 km^3, respectively. The intersection of these salinity and temperature ranges resulted in an estimated 65.2 km^3 of optimal habitat in the bay. The regions of predicted optimal habitat were plotted in Fig. 8. As demonstrated by Schlenger et al. (2013b), system-wide habitat volumes can be calculated daily and can be integrated to derive seasonal and annual totals that allow interannual comparisons in habitat volume based on predictions from coupled circulation and biogeochemical models.

3. Summary and Discussion

The novel Pentahedron method was developed to calculate analytically the volume of irregularly shaped grid cells formed with the rho nodes of an Arakawa C-grid from circulation or coupled circulation and biogeochemical models. In addition, the Pentahedron method was readily adapted to calculate the volume of the portion of a grid cell that qualified as suitable habitat for a species of interest, including when rho nodes were specified as land or when no suitable habitat was predicted at a location. The example of calculating the optimal habitat of juvenile striped bass using HabVol illustrated the utility of the method (Fig. 8), as did the extensive analyses presented by Schlenger et al. (2013b) who used more complex criteria for defining habitat suitability.

Although certainly many more factors beyond habitat volume influence the survival, growth, and distribution of living marine resources (e.g., food availability and predation), the ability to calculate and compare changes in physically-defined habitat is an important step forward for better understanding the physical drivers of range-shifts and changes in abundance. Previous modeling studies have estimated changes in abundance and distribution of species due to habitat variability, but few calculate habitat volume variations, which offer a robust metric of environmental favorability for a species (Gotelli and Ellison, 2006; Kimmerer et al., 2009; Werner et al., 2001). The Pentahedron method described here could be applied for any 3D circulation and coupled bio-physical model that predicts a suite of changing physical conditions relevant to a species. Habitat volumes calculated with historical predictions could reveal mechanisms that may have affected population growth or population decline in various species. When run with future projections exploring the influence of climate change or nutrient loading, changes in habitat volumes could be used to identify sensitive species, providing information useful for fisheries and water quality managers. Furthermore, the metrics calculated using this habitat volume method could be used as habitat forcing functions in models such as Ecopath (Christensen and Walters, 2004). Thus, the approach presented here could link circulation models that have no living resources but high resolution to upper trophic level models with many species but low physical resolution and could have wide application to the computational tools that support fisheries management.

Acknowledgements

We would like to thank to Adam J. Schlenger for assistance with information on striped bass tolerances and David H. Secor for his advice on an earlier version of this manuscript. We would also like to thank our three anonymous reviewers whose insightful comments helped to greatly improve this manuscript. This research was supported by a grant from the U.S. National Oceanic and Atmospheric Administration (NOAA) Coastal Hypoxia Research Program (CHRP) (NA07NOS4780191). This is UMCES Contribution number HPL-xxxxxx.

Literature Cited

Allen, J. S., Newberger, P. A., Federiuk, J., 1995. Upwelling Circulation on the Oregon Continental Shelf. Part I: Response to Idealized Forcing. Journal of Physical Oceanography 25, 1843–1866.

Barnes, T. K., Volety, A. K., Chartier, K., Mazzotti, F. J., Pearlstine, L., 2007. A habitat suitability index model for the easter oyster (*Crassostrea virginica*), a tool for restoration of the Chaloosahatchee Estuary, Florida. Journal of Shellfish Research 26(4), 949–959.

Bidegain, G., Bárcena, J. F., García, A., Juanes, J. A., 2013. LARVAHS: Predicting clam larval dispersal and recruitment using habitat suitability-based particle tracking model. Ecological Modelling 268, 78–92.

Blumberg, A. F., Mellor, G. L., 1987. A description of a three-dimensional coastal ocean circulation model. In Heaps, N. (ed.), Three-Dimensional Coastal Ocean Models, Volume 4. American Geophysical Union: Washington, D.C., 1–16.

Brandt, S.B., 1993. The effect of thermal fronts on fish growth: A bioenergetics evaluation of food and temperature. Estuaries 16, 142–159.

Breitburg, D. L., 1994. Behavioral response of fish larvae to low dissolved oxygen concentrations in a stratified water column. Marine Biology 120, 615–625.

Caddy, J. F., 1993. Toward a comparative evaluation of human impacts on fishery ecosystems of enclosed and semi-enclosed seas. Reviews in Fisheries Science 1, 57–95.

Caldeira, K., Wickett, M. E., 2003. Anthropogenic carbon and ocean pH. Nature 425, 365–365.

Cerco, C., 1995. Simulation of long-term trends in Chesapeake Bay Eutrophication. Journal of Environmental Engineering (ASCE) 121, 298–310.

Christensen, V., Walters, D. J., 2004. Ecopath with Ecosim: Methods, capabilities and limitations. Ecological Modelling 172, 109–139.

Cline, T. J., Bennington, V., Kitchell, J. F., 2013. Climate Change Expands the Spatial Extent and Duration of Preferred Thermal Habitat for Lake Superior Fishes. PLoS One 8, e62279.

Diaz, R. J., Rosenberg, R., 1995. Marine benthic hypoxia: A review of its ecological effects and the behavioral responses of benthic macrofauna. Oceanography and Marine Biology: An annual Review 33, 245–303.

Ezer, T., Mellor, G. L., 1994. Diagnostic and prognostic calculations of the North-Atlantic circulation and sea-level using a sigma-coordinate ocean model. Journal of Geophysical Research–Oceans 99(C7), 14159–14171.

Farin, G., 1996. Curves and Surfaces for Computer Aided Geometric Design 4th ed. Academic Press, New York, 429pp.

Funderburk, S. L., Jordan, S. J., Mihursky, J. A., Riley, D. (eds.), 1991. Habitat Requirements for Chesapeake Bay Living Resources. Chesapeake Bay Program, Annapolis, MD.

Gotelli, N. J., Ellison, A. M., 2006. Food-web models predict species abundances in response to habitat change. PLoS Biology 4, 1869–1873.

Hanks, D. M., Secor, D. H., 2011. Bioenergetic responses of Chesapeake Bay white perch (*Morone americana*) to nursery conditions of temperature, dissolved oxygen, and salinity. Mar Biol 158, 805–815.

Harley, C. D. G., Hughes, A. R., Hultgren, K. M., Miner, B. G., Sorte, C. J. B., Thornber, C. S., Rodriguez, L. F., Tomanek, L., Williams, S. L., 2006. The impacts of climate change in coastal marine systems. Ecology Letters 9(2), 228–241.

Holloway, P. E., Merrifield, M. A., 1999. Internal tide generation by seamounts, ridges, and islands. Journal of Geophysical Research 104, 25937–25951.

IPCC, 2007. Climate Change 2007: The Physical Science Basis. Contribution of Working Group I to the Fourth Assessment Report of the Intergovernmental Panel on Climate Change. S. Solomon *et al.*, Eds. Cambridge Univ. Press, Cambridge, UK, and New York.

Karlson, K., Rosenberg, R., Bonsdorff, E., 2002. Temporal and spatial large-scale effects of eutrophication and oxygen deficiency on benthic fauna in Scandinavian and Baltic waters – A review. Oceanography and Marine Biology 40, 427–489.

Kemp, W. M., Boynton, W. R., Adolf, J. E., Boesch, D. F., Boicourt, W. C., Brush, G., Cornwell, J. C., Fisher, T. R., Glibert, P. M., Hagy, J. D., Harding, L., Houde, E. D., Kimmel, D., Miller, W., Newell, R. I. E., Roman, M. R., Smith, E. M., Stevenson, J. C., 2005. Eutrophication of Chesapeake Bay: Historical trends and ecological interactions. Marine Ecology Progress Series 303, 1–29.

Kimmerer, W. J., Gross, E. S., MacWilliams, M. L., 2009. Is the response of estuarine nekton to freshwater flow in the San Francisco Estuary explained by variation in habitat volume? Estuaries and Coasts 32(2), 375–389.

Kimmerer, W. J., MacWilliams, M. L., Gross, E. S., 2013. Variation of Fish Habitat and Extent of the Low-Salinity Zone with Freshwater Flow in the San Francisco Estuary. San Fr. Estuary Watershed Sci. 11, 1–16.

Kremer, J. N., Nixon, S. W., 1978. A coastal marine ecosystem. Simulation and analysis. Springer-Verlag, Berlin, 217 pp.

Li, M., Lee, Y. J., Testa, J. M., Li, Y., Kemp, W. M., Di Toro, D. M., 2016. What drives interannual variability of hypoxia in Chesapeake Bay: Climate forcing versus nutrient loading? Geophysical Research Letters, 43, 2127–2134, doi:10.1002/2015GL067334.

Li. M,, Zhong, L., Boicourt, W.C., 2005. Simulations of the Chesapeake Bay estuary: sensitivity to turbulence mixing parameterization and comparison with hydrographic observations. *J. Geophys. Res.* 110, C12004, doi:10.1029/2004JC002585.

MacWilliams, M., Bever, A. J., Foresman, E., 2016. 3-D simulations of the San Francisco Estuary with subgrid bathymetry to explore long-term trends in salinity distribution and fish abundance. San Fr. Estuary Watershed Sci. 14(2): 3.

Mann, K. H., Lazier, J. R. N., 2006. Dynamics of Marine Ecosystems: Biological-Physical Interactions in the Oceans, 3rd ed. Blackwell Publishing, Oxford, 496 pp.

McLeese, D., 1956. Effects of temperature, salinity and oxygen on the survival of the American lobster. J Fish Res Board Can 13, 247–272.

Miller, D. C., Poucher, S. L., Coiro, L., 2002. Determination of lethal dissolved oxygen levels for selected marine and estuarine fishes, crustaceans, and a bivalve. Marine Biology 140, 287–296.

Mouton, A., Meixner, H., Goethals, P. L. M., De Pauw, N., Mader, H. 2007. Concept and application of the usable volume for modeling the physical habitat of riverine organisms. River Research and Applications 23(5), 545–558. doi:10.1002/rra.998

Nixon, S. W., 1995. Coastal marine eutrophication: A definition, social causes, and future concerns. Ophelia 41, 199–219.

Peeters, J., Los, F., Hansen, R., Haas, H., Peperzak, L., de Vries, I., 1995. The oxygen dynamics of the oyster ground, North Sea. Impact of eutrophication and environmental conditions. Ophelia 42, 257–288.

R Development Core Team, 2005. R: A language and environment for statistical computing. R Foundation for Statistical Computing, Vienna, Austria. ISBN 3-900051-07-0, URL http://www.R-project.org.

Scavia, D., Field, J. C., Boesch, D. F., Buddemeier, R. W., Burkett, V., Cayan, D. R., Fogarty, M., Harwell, M. A., Howarth, R. W., Mason, C., Reed, D. J., Royer, T. C., Sallenger, A. H., Titus, J. G., 2002. Climate change impacts on U.S. coastal and marine ecosystems. Estuaries 25(2),149–164.

Schlenger, A. J., 2012. Modeling potential habitat of Chesapeake Bay living resources. Masters Thesis, University of Maryland College Park, College Park, Maryland, USA, 209 pp.

Schlenger, A. J., Schlag, Z.,, North, E. W., 2013a. Habitat Volume Model (HabVol) User's Guide. University of Maryland Center for Environmental Science, Horn Point Laboratory. Cambridge, MD. 14 pp. Downloaded on 9/28/2017 from http://northweb.hpl.umces.edu/open_source_code/HabitatVolumeModel.htm

Schlenger, A. J., North, E. W., Schlag, Z., Li, Y., Secor, D. H., Smith, K. A., Niklitschek, E. J., 2013b. Modeling the influence of hypoxia on the potential habitat of Atlantic sturgeon (*Acipenser oxyrinchus*): a comparison of two methods. Marine Ecology Progress Series 483, 257–272.

Secor, D. H., Gunderson, T. E., 1998. Effects of hypoxia and temperature on survival, growth, and respiration of juvenile Atlantic sturgeon (*Acipenser oxyrinchus*). Fishery Bulletin 96, 603–613.

Song, Y. H., Haidvogel, D., 1994. A semi-implicit ocean circulation model using a generalized topography-following coordinate system. Journal of Computational Physics 115, 228–244.

Wells, D., 2012. Games and Mathematics: Subtle Connections. Cambridge University Press, New York. 246 pp.

Werner, F. E., Quinlan, J. A., Lough, R. G., Lynch, D. R., 2001. Spatially-explicit individual based modeling of marine populations: a review of the advances of the 1990s. Sarsia 86, 411–21.

Wuenschel, M. J., Jugovich A. R., Hare J. A., 2004. Effect of temperature and salinity on energetics of juvenile gray snapper (*Lutjanus griseus*): implications for nursery habitat value. J Exp Mar Biol Ecol 312, 333–347.

Yi, Y., Wang, Z., Yang, Z., 2010. Two-dimensional habitat modeling of Chinese sturgeon spawning sites. Ecological Modeling 221, 864–875.

Figures

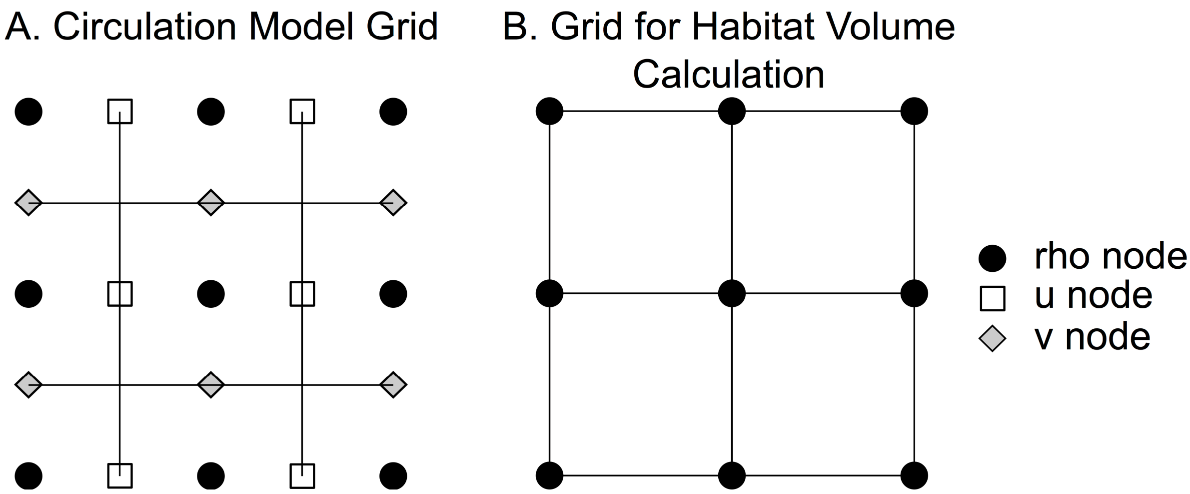

Figure 1. Plan view of the grids used for habitat volume algorithm development. A) An Arakawa C-grid structure, with rho nodes located in the center of the grid cells. Water properties like temperature and salinity are calculated at the rho nodes of circulation models that are based on the Arakawa C-grid. B) The grid structure for the habitat volume calculations herein. This grid employed the rho nodes from the circulation model as the vertices of its grid cells. Note that the grids are depicted here as rectilinear, which was not a property required for volume calculations.

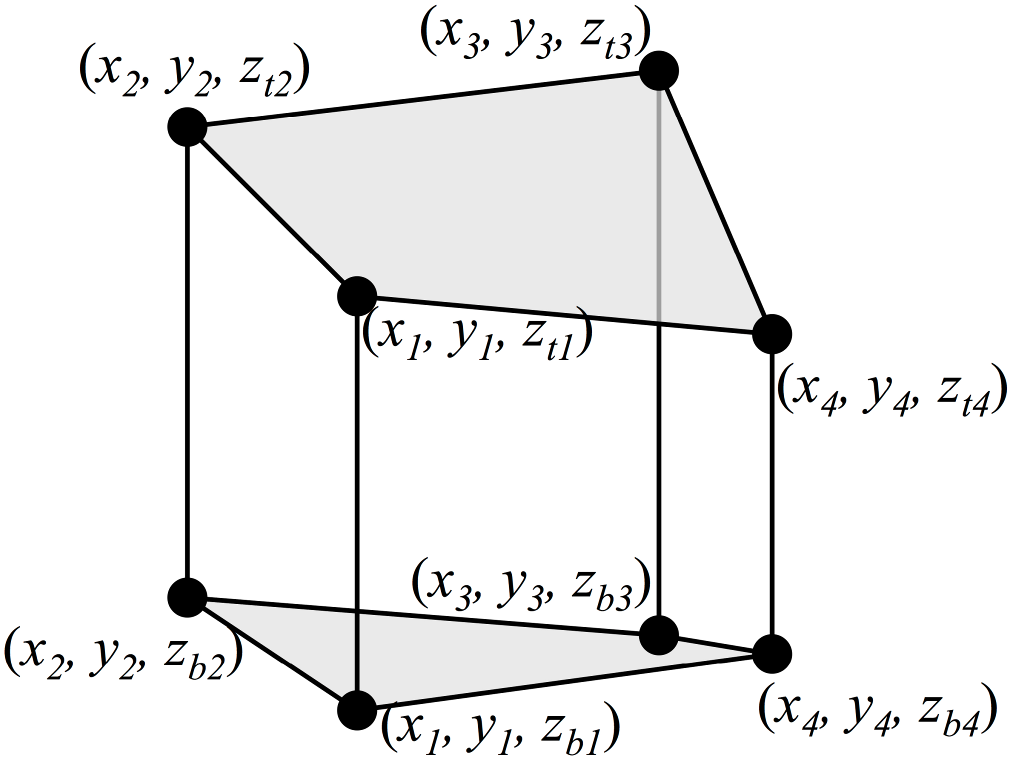

Figure 2. An example of a grid cell used for calculating habitat volume with the top (*t*) and bottom (*b*) vertices labeled. The top and bottom faces were not necessarily planar and thus can form skew quadrilaterals.

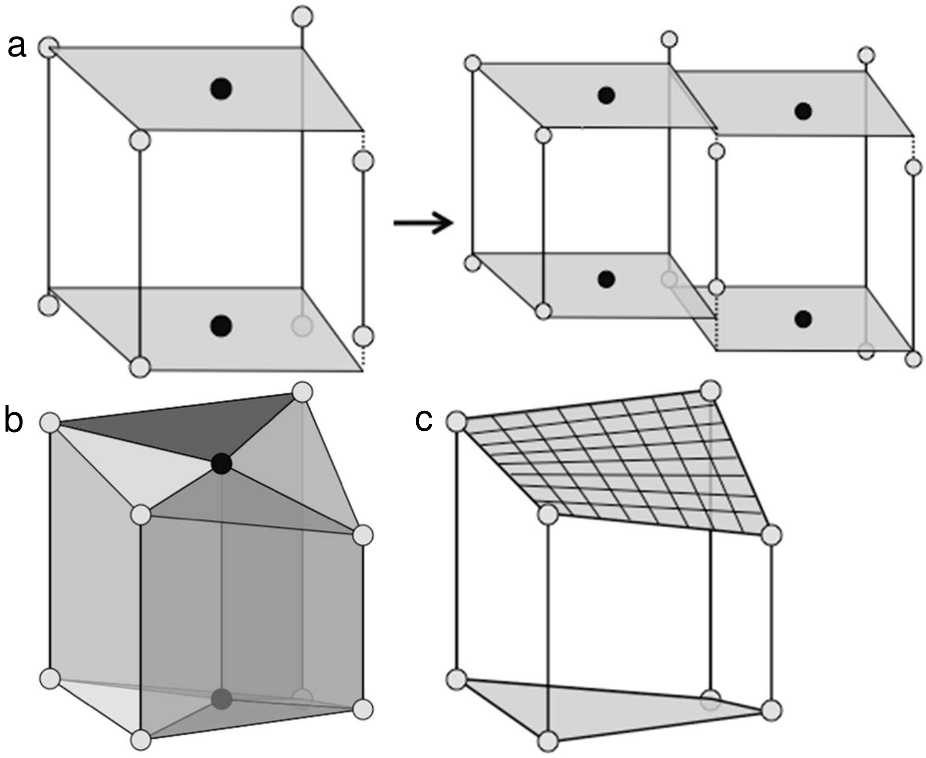

Figure 3. Schematic of three methods used to define volume based on an Arakawa C-grid. a) Step method. Top and bottom faces (gray surfaces) were assumed to be flat and were placed horizontally at the heights of the midpoints (black circles) of the top and bottom cell vertices (gray circles), respectively. This method led to discontinuities between adjacent cell volumes. b) Pentahedron method. Top and bottom faces were each defined by the four triangles that can be formed with two adjacent grid cell vertices and the face midpoint. Corresponding top and bottom triangles were connected vertically to form four pentahedrons. c) Ruled Surface method. Top and bottom faces were defined as the hyperbolic paraboloids formed by the skew quadrilaterals joining the four top and four bottom vertices, respectively. These were constructed by connecting the midpoints of opposite sides of a face, then connecting opposite quarter points, etc., until the surface was filled out. A few such lines are illustrated on the top face.

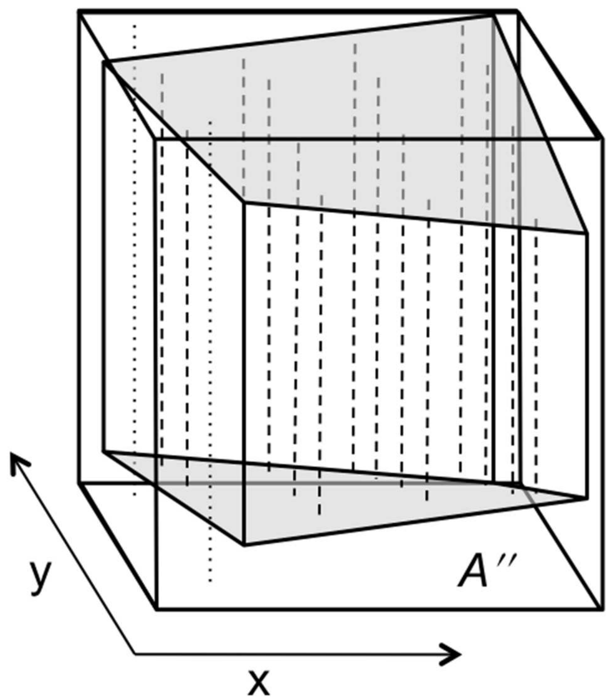

Figure 4. Schematic of the Ruled Surface method to calculate volume of a three-dimensional cell with top and/or bottom faces defined as hyperbolic paraboloid (ruled) surfaces. A box with rectangular faces was constructed around the cell with its corner points defined by the extremes of the cell’s vertices. Heights of the cell (dashed lines) were sampled at regularly spaced horizontal locations throughout the box, and points that were completely outside the cell (dotted lines) were counted as having a height of zero. The average of all sampled heights was then multiplied by the area (A'') of the rectangular box’s horizontal face to give the volume estimate.

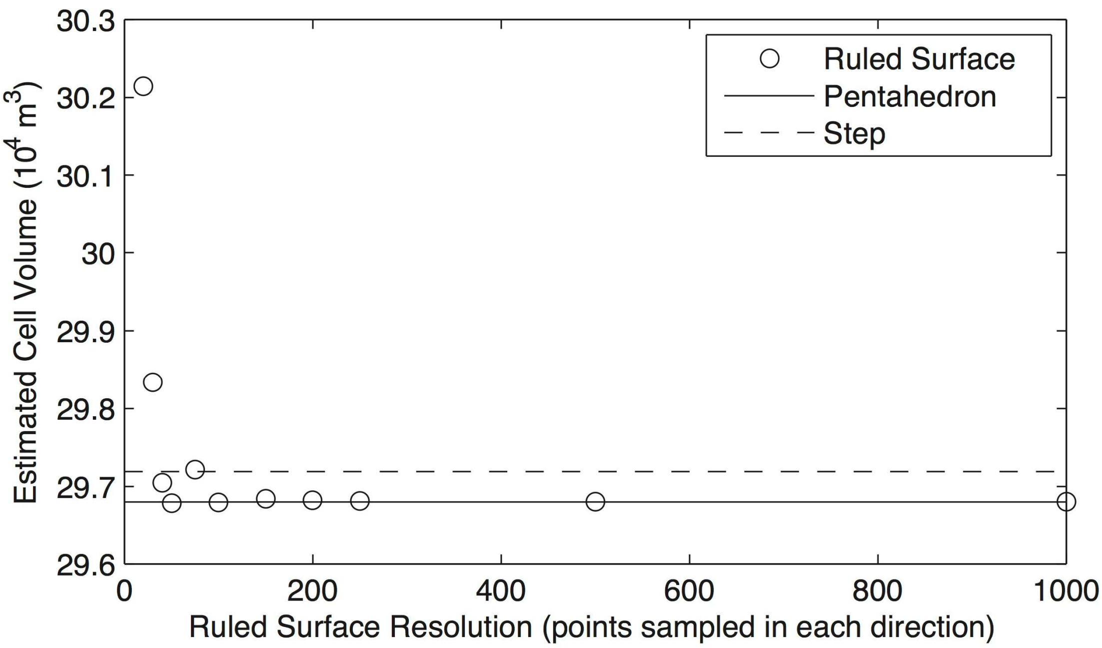

Figure 5. The volume of a sample grid cell calculated using the Ruled Surface method with increasing numerical resolution (the number of points sampled in both the *x* and *y* directions), compared with the volume calculated using the Pentahedron and Step methods. As the number of *x-y* points used for the Ruled Surface method increased, the Ruled Surface solution converged with the Pentahedron solution.

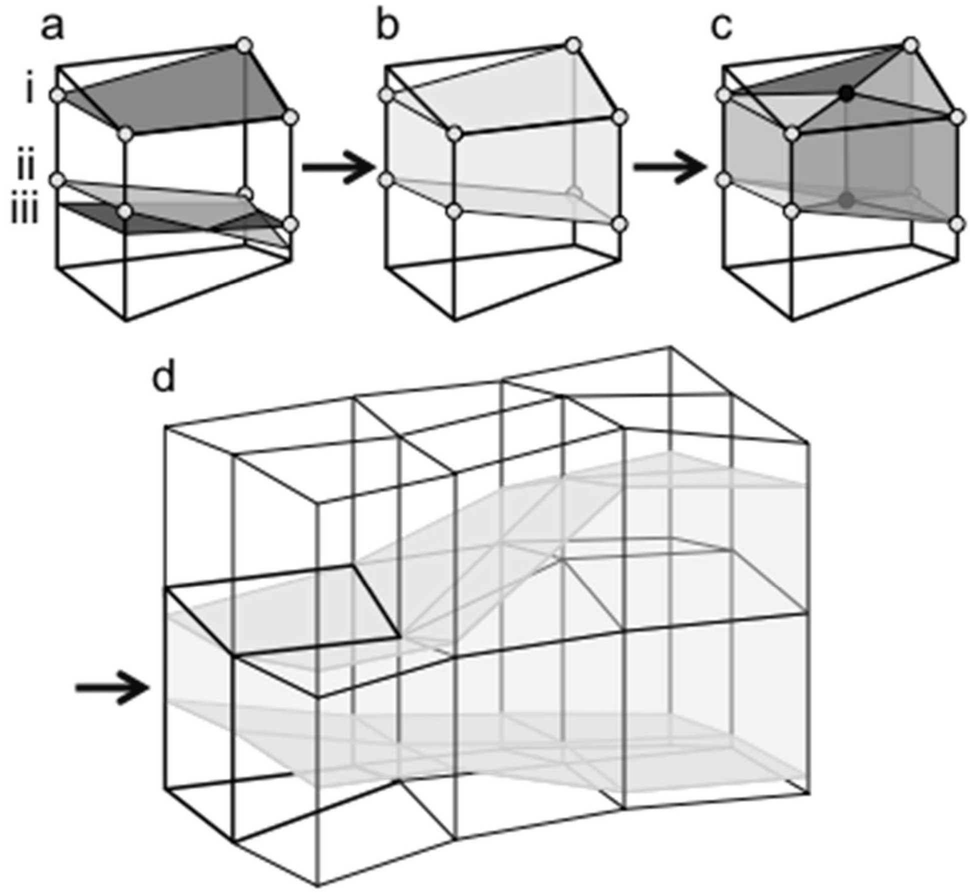

Figure 6. Conceptual schematic of habitat volume calculation based on multiple physiological constraints. a) Linear interpolation in the vertical was used to find an upper boundary for salinity (i), lower boundary for dissolved oxygen (ii), and lower boundary for temperature (iii) based on a species' tolerances. b) The most constraining boundary points were chosen (gray circles) to define the suitable habitat in the grid cell. c) The suitable habitat region was divided into four pentahedrons, according to the Pentahedron method, and its volume was calculated as the sum of the volumes of the pentahedrons. d) The process was repeated for every grid cell in the model, and the volumes were summed to calculate the model-wide habitat volume.

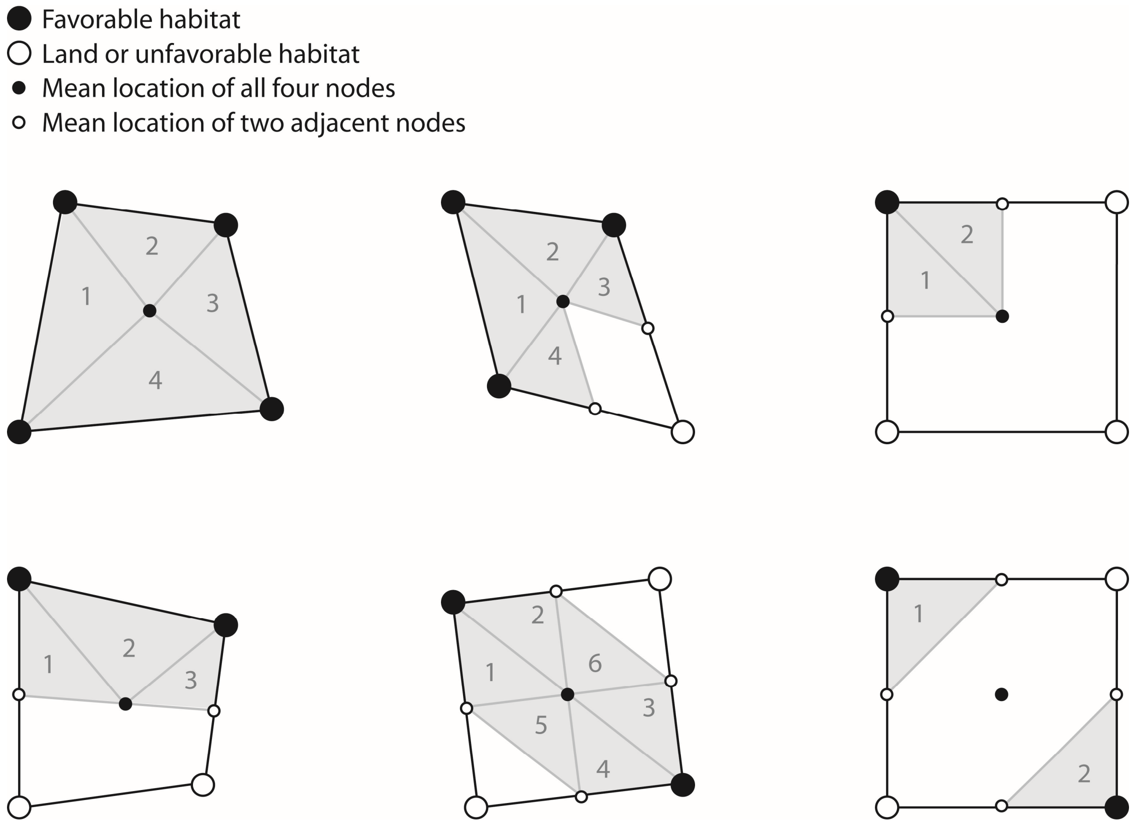

Figure 7. Diagram of the application of the Pentahedron method for calculating volume (gray areas) based on rho nodes (large circles at quadrilateral corners) from an Arakawa C-grid. Six cases are represented: when all rho nodes were water (large black circles) and favorable habitat was defined at all four nodes (upper left quadrilateral) and special cases near the land boundaries or when suitable habitat did not exist at all nodes (large white circles in the remaining cases). Numbered triangles inside each quadrilateral indicate the areas in which the Pentahedron method was applied to calculate the volume in that water column. Small white circles indicate half the distance between the rho nodes.

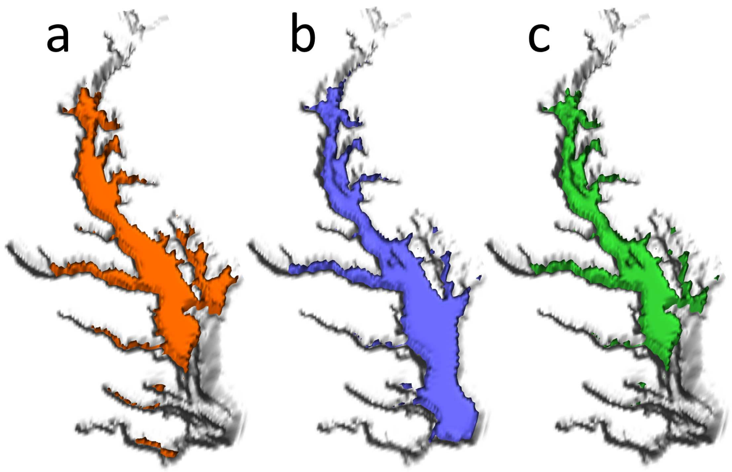

Figure 8. Example predictions of optimal habitat from the Habitat Volume Model using the Pentahedron method. Each panel depicts the location of optimal habitat for juvenile striped bass (*Morone saxatilis*) on August 15, 1996 based on the physiological tolerance thresholds for a) salinity (orange), b) temperature (blue) and c) combined salinity and temperature (green). The salinity and temperature thresholds were set to 1–15 and 24–27 °C, respectively, based on a literature review in Schlenger (2012).